

Experimental demonstration of tokamak inductive flux saving by transient coaxial helicity injection on national spherical torus experiment^{a)}

R. Raman,^{1,b),c)} D. Mueller,² T. R. Jarboe,¹ B. A. Nelson,¹ M. G. Bell,² S. Gerhardt,² B. LeBlanc,² J. Menard,² M. Ono,² L. Roquemore,² and V. Soukhanovskii³

¹University of Washington, Seattle, Washington 98195, USA

²Princeton Plasma Physics Laboratory, Princeton, New Jersey 08543, USA

³Lawrence Livermore National Laboratory, Livermore, California 94551, USA

(Received 13 June 2011; accepted 5 August 2011; published online 6 September 2011)

Discharges initiated by transient coaxial helicity injection in National Spherical Torus Experiment have attained peak toroidal plasma currents up to 300 kA. When induction from the central solenoid is then applied, these discharges develop up to 300 kA additional current compared to discharges initiated by induction only. CHI initiated discharges in NSTX have achieved 1 MA of plasma current using only 258 mWb of solenoid flux whereas standard induction-only discharges require about 50% more solenoid flux to reach 1 MA. In addition, the CHI-initiated discharge has lower plasma density and a low normalized internal plasma inductance of 0.35, as needed for achieving advanced scenarios in NSTX. © 2011 American Institute of Physics.

[doi:10.1063/1.3628540]

I. INTRODUCTION

Both conventional aspect ratio tokamaks and spherical tokamaks (STs) have generally relied on a central solenoid to generate the initial plasma current and then to sustain that current against resistive dissipation. However, in a steady-state reactor, a central solenoid cannot be used for plasma current sustainment. Fortunately, substantial progress in tokamak research during the past two decades has made it possible to sustain the current non-inductively for significant periods.¹ However, the inclusion of a central solenoid in a tokamak to provide plasma startup limits the minimum aspect ratio. For reactors based on the ST concept, elimination of the central solenoid is essential, making alternate methods for plasma start-up necessary for such a reactor.

The generation of toroidal plasma current by coaxial helicity injection (CHI) was originally developed for spheromak plasma formation² and has been used on several spheromak experiments including on the SSPX (Sustained Spheromak Physics Experiment), CTX (Compact Torus Experiment), and RACE (Ring Accelerator Experiment) devices.^{3–5} It has also been used in reconnection merging experiments^{6,7} and for spherical torus plasma formation.^{8,9}

The first experiments utilizing CHI on NSTX used the method of *driven* or *steady-state* CHI for plasma current initiation.⁹ However, the toroidal currents generated using this method was not successfully sustained by applying induction. Later, experiments on the HIT-II experiment at the University of Washington demonstrated that the method of *transient* CHI could generate a high-quality plasma equilibrium in a ST that could be coupled to induction.¹⁰ The transient-CHI method has now been successfully used on NSTX for solenoid-free plasma start-up followed by inductive

ramp-up.¹¹ These coupled discharges have now achieved toroidal currents >1 MA using significantly less inductive flux than standard inductive discharges in NSTX.

II. TRANSIENT CHI START-UP

As shown in Fig. 1, CHI is implemented in NSTX by driving current along field lines that connect the inner and outer lower divertor plates. The standard operating condition for CHI in NSTX uses the inner vessel and lower inner divertor plates as the cathode while the outer divertor plates and vessel are the anode. A CHI discharge is initiated by first energizing the toroidal field coils and the lower divertor coils to produce magnetic flux linking the lower inner and outer divertor plates which are electrically isolated by a toroidal insulator in the vacuum vessel. After a programmed amount of gas is injected into the vacuum chamber, a voltage is applied between these plates which ionizes the gas and produces current flowing along magnetic field lines connecting the plates. In NSTX, a 5–30 mF capacitor bank charged to 1.7 kV provides this current, called the injector current. As a result of the applied toroidal field, the field lines joining the electrodes wrap around the major axis many times so the injector current flowing in the plasma develops a much larger toroidal component.

If the injector current exceeds a threshold value, the resulting $J_{\text{pol}} \times B_{\text{tor}}$ stress across the current layer exceeds the field-line tension of the injector flux causing the helicity and plasma in the lower divertor region to be injected into the NSTX vessel. This is referred to as the “bubble-burst” current. Below this bubble-burst current, the field lines do not move and the injector is effectively a fixed impedance circuit. The current required to satisfy this “bubble burst” condition is given by the relation

$$I_{\text{inj}} = 2\psi_{\text{inj}}^2 / (\mu_0^2 d^2 I_{\text{TF}}). \quad (1)$$

^{a)}Paper DI3 4, Bull. Am. Phys. Soc. 55, 105 (2010).

^{b)}Invited speaker.

^{c)}Electronic mail: raman@aa.washington.edu.

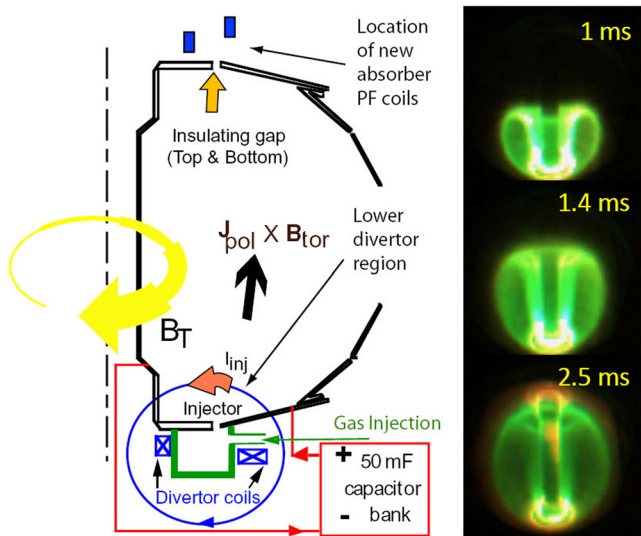


FIG. 1. (Color online) Schematic drawing of the NSTX machine components including the location of the insulating gaps between the divertor plates, the lower divertor coils used for generating the CHI injector flux, and the absorber poloidal field coils. Shown on the right are fast camera fish eye images of an evolving CHI discharge at 1, 1.4, and 2.5 ms after discharge initiation time.

Here ψ_{inj} is the poloidal flux at the injector insulating gap, I_{TF} is the total current in the toroidal field coil, and d is the gap between the injector flux “footprints” on the electrodes.¹² In NSTX, the lower divertor electrodes are referred to as the “injector” and the similarly insulated upper divertor plates are referred to as the “absorber.” The $E \times B$ plasma drift is away from the injector region and towards the absorber region.

To estimate the toroidal current produced by CHI, we define the quantities $\lambda_{inj} = \mu_0 I_{inj} / \psi_{inj}$ and $\lambda_{tokamak} = \mu_0 I_p / \phi_{wall}$, where ϕ_{wall} is the toroidal flux contained in the plasma poloidal cross-section. By considering the generation of magnetic helicity during CHI, it can be shown that $\lambda_{inj} > \lambda_{tokamak}$,¹² so that

$$I_p \leq I_{inj} \left(\frac{\phi_{wall}}{\psi_{inj}} \right). \quad (2)$$

In NSTX, the magnitude of the toroidal plasma current during CHI is typically 50–70 times that of the injected current.

If, after the plasma fully fills the vessel, the injector current is rapidly reduced below the bubble-burst threshold, the plasma disconnects from the injector to form a closed field line configuration which can retain a significant toroidal current. However, if the expanding CHI-produced plasma reaches the (upper) absorber structure while voltage is still being applied across the electrodes, a secondary discharge can develop in the absorber. This is referred to as an “absorber arc” and it can present a much lower impedance than the injector.

The fast camera images in Fig. 1 show that the growth of the CHI discharge is very rapid. About 2.5 ms after discharge initiation, approximately 300 kA of toroidal current is generated. The initial energy stored in the capacitor bank is about 29 kJ resulting in a remarkable current generation efficiency of 10 A/J.

The CHI drives current initially on open field lines creating a toroidal current density profile in the poloidal (R-Z) plane that is hollow. Taylor relaxation¹³ predicts a flattening of this current profile through a process of magnetic reconnection leading to current flowing throughout the volume, including on closed field lines. Current penetration to the interior is needed for usefully coupling CHI to other current drive methods or for CHI to sustain current during an extended non-inductive phase. It is the toroidal plasma current component flowing along closed field lines after the injected current has been terminated that can be subsequently driven inductively to increase its magnitude.

The driven or steady-state method of CHI relies on the development of non-axisymmetric plasma perturbations to drive current on closed flux surfaces. During this mode of CHI operation, the CHI injector circuit is continuously driven for some time ($t_{pulse} > t_{L/R}$). The more recent *transient* CHI approach involves a nearly axisymmetric reconnection. This method has now been successfully used for the generation of a closed flux equilibrium which could be coupled to induction.

This paper describes new results in which the CHI-produced toroidal plasma current up to ~ 0.3 MA was ramped up to 1 MA using 40% less central solenoid flux than required by standard startup involving only induction. In addition, the discharges that involved CHI start-up had lower electron density, lower internal plasma inductance, and high elongation from very early in the discharge. These properties of the resulting discharges are eventually needed for achieving advanced scenarios in NSTX and its planned upgrade NSTX-U.¹⁴

III. EXPERIMENTAL RESULTS

The results reported in this paper were made possible by reductions to the low-Z impurities, mainly oxygen and carbon, as described in Ref. 11 and briefly summarized here.

First, it was necessary to clean the lower divertor plates, which function as the CHI electrodes. This was accomplished by running several discharges at high injector current levels but with increased poloidal flux connecting the lower divertor plates (the injector flux) to raise the bubble-burst current (Eq. (1)) so that the discharge stayed connected to the lower divertor plates. Then, the lower divertor plates were coated with lithium by a pair of evaporator ovens mounted at the top of the vacuum chamber.¹⁵ These evaporators directed collimated streams of lithium vapor onto the lower divertor plates and the surrounding plasma-facing surfaces between plasma discharges. Typically, 100–200 mg of lithium was applied before each CHI discharge producing a lithium coating 10–50 nm thick on the electrode surfaces. Third, two poloidal field coils located in the upper divertor region were energized to provide a “buffer” flux to reduce contact of the growing CHI discharge with the upper divertor electrodes. In the absence of this buffer flux, once the CHI discharge contacted the upper (absorber) divertor electrodes, a pronounced absorber arc usually developed which generated low-Z impurities causing the CHI initiated discharge to become more resistive which rapidly consumed the poloidal flux generated in the plasma.

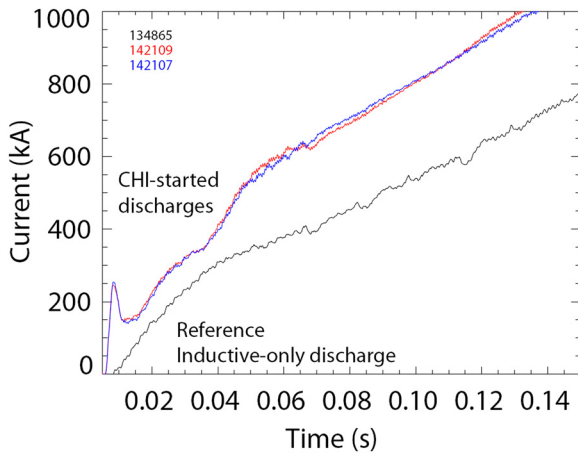


FIG. 2. (Color online) Shown are the plasma currents for two discharges initiated using CHI startup and ramped up using the central solenoid. The black trace is for a reference inductive only discharge that remained in L-mode and ramped up to 1 MA in the shortest possible time. At 130 ms, the CHI started discharges have ramped up to 1 MA whereas the inductive discharge that has used the same amount of inductive flux has ramped to a lower value of 700 kA.

Fig. 2 shows two CHI started discharges that were coupled to induction. The third discharge is an inductive-only case that is a non-CHI discharge from the NSTX database (assembled over 10 yr of operation) that reached 1 MA in a shorter time than other L mode discharges. For the CHI initiated discharge at 132 ms, a total of 258 mWb of central solenoid flux was required to ramp the discharge to 1 MA. The non-CHI discharges at this time only gets to about 0.7 MA and does not reach 1 MA until 160 ms, by which time 396 mWb of central solenoid flux had been consumed. Thus, the L-mode discharges from the NSTX data base require at least 50% more inductive flux than discharges assisted by CHI. The discharge on NSTX that consumed the least amount of solenoid flux to reach 1 MA transitioned to an H mode. That discharge required 340 mWb to reach 1 MA, which is still significantly higher than the CHI started discharges.

In Fig. 3, we show other parameters for discharges started with and without CHI. The CHI assisted discharges have much lower plasma internal inductance and their line-integral electron density is about one third that of the standard NSTX discharges. As a result of the lower inductance, the CHI started discharges also have a higher plasma elongation for a similar programming of the NSTX shaping coils. The CHI assisted discharge 142140 has a higher electron density than discharges 140872 and 140875, starting from 80 ms, due to increased gas puffing.

These recent CHI discharges have lower electron density than is typically produced by the standard inductive startup in NSTX. Early CHI discharges in NSTX had higher density as a result of the large amount of gas injected into the main chamber to produce the pressure needed to achieve reliable breakdown between the CHI electrodes. To reduce the amount of gas required, the location of gas injection was changed from ports on the lower inner divertor plates to the small cavity below the lower divertor plates so that the gas emerged from the narrow (~ 2 cm) annular gap between the CHI electrodes. A sufficiently high pressure could then be

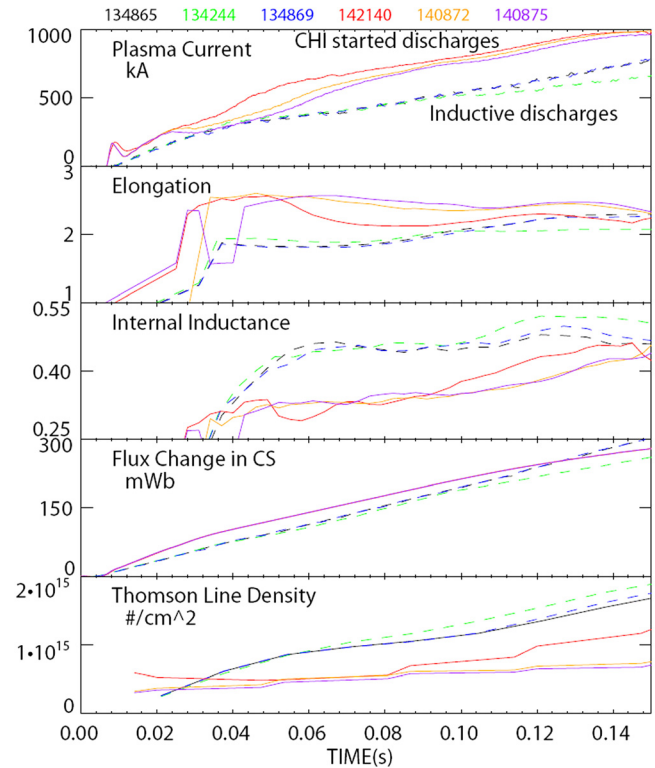


FIG. 3. (Color online) (From top to bottom) Time traces for the plasma current, plasma elongation, normalized plasma internal inductance, flux change in the central solenoid, and the electron line density from a Thomson scattering diagnostic. The traces are for three discharges initiated using CHI startup (142140, 140872, and 140875) and three reference inductive-only discharges (shown by the dashed lines) that ramped to 1 MA in the shortest possible time.

achieved transiently in the gap between electrodes to allow gas breakdown with a reduced total amount of injected gas. Initially, about 10 kW of 18 GHz electron cyclotron resonance heating power was also injected into the chamber below the lower divertor plates to ionize the injected gas. However, it was subsequently determined that even without the ECRH system, the discharge initiation was quite reliable with total deuterium gas injection of only about 2 Torr l into the lower cavity. This is similar to the amount injected as pre-fill for standard inductive plasma generation. A further important aspect of these CHI generated discharges is that they can be inductively ramped up without any additional gas injection during the inductive ramp.

We note from the traces showing the change in the flux change produced by the central solenoid that initially the CHI started discharges consume more inductive flux. This is because they are initiated using an electrode discharge, so have relatively more low-Z impurities than discharges started by purely inductive means. As a result these discharges require some additional input power to burn through the low-Z impurities. For the CHI started discharges, the initial loop voltage is about 3 V for 20 ms while the plasma current is about 200 kA, which results in a modest input power of 600 kW. In future, devices auxiliary heating power of this magnitude for about 20 ms, such as from ECRH, should be able to boost the electron temperature and reduce plasma resistivity. However, past this initial time the loop voltage

consumed by the CHI discharge drops below the level in the non-CHI discharge. At about 120 ms, the inductive flux usage by both discharges becomes equal. Beyond 120 ms, the flux usage by the CHI discharge drops rapidly because the CHI discharge uses a unipolar central solenoid swing with a maximum available flux of 330 mWb. The non-CHI discharges use a bipolar swing and so have twice as much flux available (660 mWb). At 150 ms, the loop voltage for the CHI started discharges becomes too low to sustain these 1 MA plasmas. The drop in the applied loop voltage is also the reason for the gradual increase in the internal inductance after 120 ms.

Operational experience has shown that for the standard inductive startup in NSTX, both the higher plasma density and the slower current ramp rates of the discharges in Fig. 3 are required to avoid MHD instability during the current ramp. The CHI started discharges seem immune to this, although the reasons for this are not known at this time. It could be related to the hollow electron temperature profile, shown in Fig. 4, that is, characteristic of CHI startup. Recall from the introductory section that initially CHI drives all current in the edge region of the plasma. After flux closure, it could then be expected that most of the current still flows at the edge until current relaxation causes the edge current to diffuse to the interior. This initially hollow current profile should result in a higher edge temperature and relatively cooler plasma center. This is indeed seen in the CHI started discharges as shown in Fig. 4. This hollow electron temperature profile persists during the subsequent inductive ramp, which causes more of the current to flow in the outer region resulting in a lower inductance plasma. This is advantageous for producing shaped equilibria because the current flowing in the plasma is effectively closer to the currents in the external equilibrium control coils. In particular, highly elongated plasmas with centrally peaked current profiles (high internal inductance) are much more susceptible to vertical displacement events than those with hollow current profiles (low inductance). Furthermore, many advanced operating modes for tokamaks strive to maintain a hollow current profile throughout the discharge both to reduce thermal transport and to maintain

macroscopic plasma stability. This is typically achieved by early plasma heating to increase the electron temperature, particularly near the edge, to lengthen the current diffusion time. That CHI is able to provide an initial current profile similar to that which is achieved in conventional tokamaks through the use of high-power auxiliary heating is an important benefit that should assist advanced scenario operations.

Another beneficial aspect of the CHI started discharges is their lower electron density. Because the energetic neutral-beam ions take a longer time to slow down in lower density discharges, the neutral beam current drive fraction increases. Low density targets are thus a requirement for ramping up an initial current to the desired steady-state current levels. NSTX-U will rely on reduced density to increase the neutral beam current drive fraction.¹⁴

Fig. 5 shows a representative CHI-only discharge (142163) that attained a peak current of 0.3 MA and two

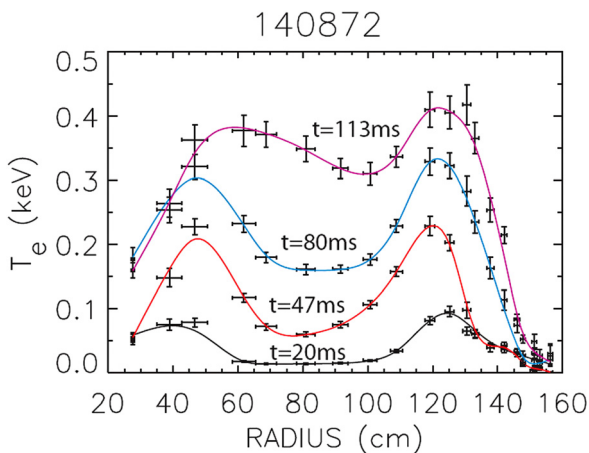


FIG. 4. (Color online) Electron temperature profiles at $t=20$, 47, 80, and 113 ms for a CHI started discharge that was inductively ramped up. The initial hollow electron temperature profile is retained during the current ramp.

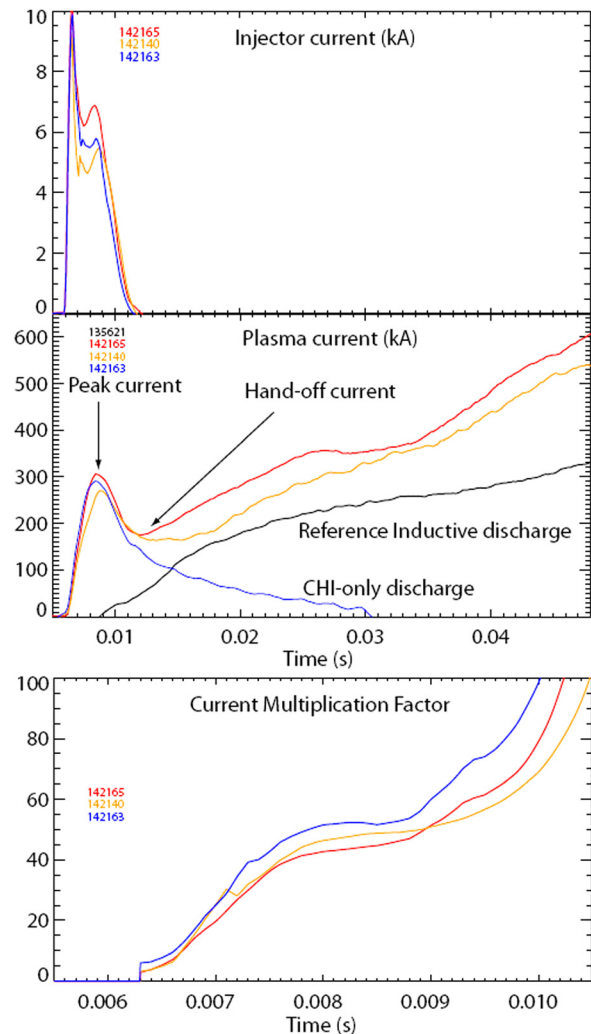


FIG. 5. (Color online) Top—Injector current traces for CHI started discharges. Middle—Plasma current traces for a CHI-only discharge (142163), CHI started discharges that were ramped up using induction (142165 and 142140) and for a reference inductive-only discharge that had the same inductive loop voltage programming as the CHI discharges that were ramped up using induction. The initial peak startup currents are 300 kA and when induction is applied, the CHI started discharge ramps up to over 600 kA, whereas the inductive-only discharge reaches about 300 kA. Bottom—Current multiplication factors for the three CHI discharges.

similar discharges (142140 and 142165) with induction also applied. The fourth discharge (135621) is an inductive-only discharge that used the same loop voltage programming as discharge 142165. By about 45 ms, the CHI started discharge reaches a current about 0.3 MA more than the reference inductive-only discharge. The initial energy stored in the capacitor bank was 29 kJ resulting in a current generation efficiency of over 10 A/J. The current multiplication factor defined as the ratio of the plasma current to the injector current is over 50.

IV. DISCUSSION AND IMPLICATIONS FOR NSTX-U

CHI started discharges that have induction applied, both on HIT-II and on NSTX, generally show a drop in plasma current before the current eventually begins to ramp-up. The lowest current during the current ramp is referred to as the hand-off current, as shown in Fig. 5.

The magnitude of this drop can be as small as 10% but generally it is about 30%. There are two reasons for this. The first is the plasma resistivity. Reducing the impurities further would reduce the plasma resistivity through decreasing the Z_{eff} and reducing the radiated power which suppresses the electron temperature. Auxiliary heating could also overcome the effects of any residual low-Z impurities.

The second reason for the current drop is the increase in plasma inductance as the initially hollow and, therefore, low inductance, current profile naturally evolves. Assuming internal flux conservation, the ratio of the initial peak current to the hand-off current provides a lower bound on the initial inductance of the CHI started plasma at the time of peak startup current. Soon after coupling to induction, the normalized plasma internal inductance of about 0.35 computed by the EFIT (Equilibrium fitting code) code analysis of the external magnetic data for these discharges is maintained through most of the inductive ramp, until the loop voltage becomes too small to sustain the plasma current. A calculation at a single time point using a second equilibrium reconstruction code LRDFIT (LR circuit model with Data Fitting capabilities) that includes a fitting constraint on the internal magnetic field line pitch measured by the Motional Stark Effect diagnostic¹⁶ gives a similar value for the plasma internal inductance. The poloidal flux corresponding to this plasma inductance is given as

$$\psi_p = I_p R_p l_i \mu_0 / 2. \quad (3)$$

Substituting $l_i = 0.35$ and $I_p = 165$ kA, and the EFIT computed value of the plasma major radius $R_p = 0.87$, Eq. (3) gives $\psi_p = 31.5$ mWb. In the absence of flux amplification, this is the amount of injector flux that must be injected into NSTX. Assuming that there is no poloidal flux decay due to resistive loss, the initial plasma internal inductance at the peak toroidal current of 270 kA is then 0.21 for these discharges.

At the time of peak CHI-produced toroidal current, the experimentally measured current multiplication is

$$CM_{\text{Exp}} = I_p / I_{\text{inj}} \approx 60. \quad (4)$$

We can compare this with the result of applying Eq. (2). The plasma enclosed toroidal flux is 2.68 Wb. Using the poloidal flux of 31.5 mWb calculated using Eq. (3) at the earliest time at which EFIT can be applied, the current multiplication factor would be

$$CM = \phi_T / \psi_p \approx 85. \quad (5)$$

This estimate of the current multiplication factor is higher because between the time of peak plasma current and the hand-off some of the injected poloidal flux has decayed away. This calculation also assumes that there is no dynamo activity that generates additional poloidal flux.

We can also use the difference between poloidal flux loops located on the outer edge of the inner divertor plates at the top and bottom of the machine, as shown in Fig. 6, to characterize the injector flux. This provides an upper bound of 50 mWb at the time of peak CHI-driven current. The difference between poloidal flux loops located at the inner and outer edges of the outer divertor plate, also shown in Fig. 6, which approximates the poloidal width of the plasma footprint on the electrodes provides a lower bound of 30 mWb. The range of experimental flux measurements is consistent with the poloidal flux calculation using plasma parameters in Eq. (3).

Using these equations, we can now calculate the projected values of the current multiplication factor and the toroidal current CHI could generate in the NSTX-U. The device parameters and the calculated values are listed in Table I.

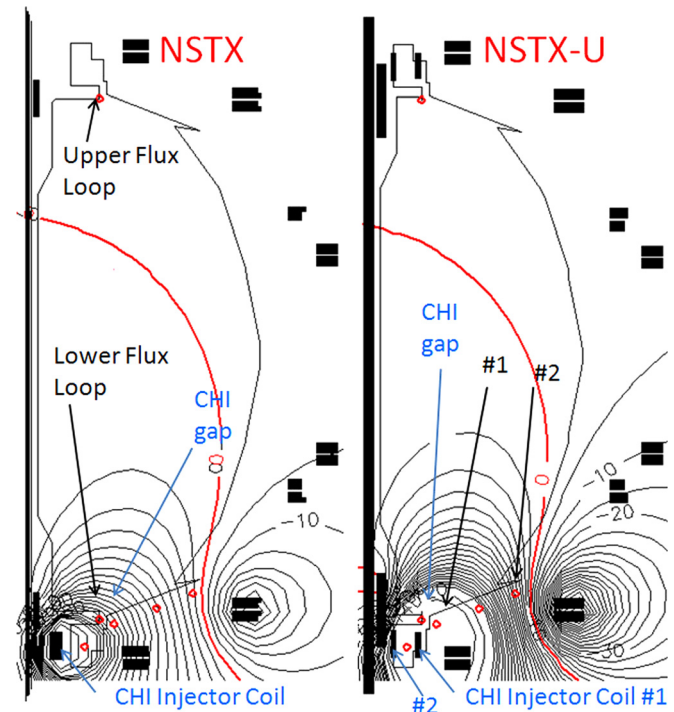


FIG. 6. (Color online) Vacuum flux calculation for NSTX and NSTX-U. For NSTX, the CHI injector coil is driven at the 10 kA limit to generate 50–80 mWb of injector flux. For NSTX-U, the injector coil #1 is driven at the 15.9 kA limit to generate over 200 mWb of injector flux. In NSTX-U, the injector coil #1 is positioned much closer to the CHI injector gap, which results in much larger injector flux. Injector coil #2 could also be used to increase the injector flux magnitude.

TABLE I. CHI startup parameters in NSTX and NSTX-U.

Parameters	NSTX	NSTX-U
R (m)	0.86	0.93
a (m)	0.68	0.62
B ₀ (T)	0.55	1.0
Toroidal flux (Wb)	2.68	3.78
Normalized internal inductance, l_i	0.35	0.35
Planned non-inductive sustainment current I_{ps} (MA)	0.7	1.0
Poloidal flux at I_{ps} (mWb)	132	206
Required injector flux for 50% I_{ps} (mWb)	66	103
Current multiplication factor for 50% I_{ps}	41	37
Peak current multiplication for 50% I_{ps}	53	48
Peak startup current (MA) for 50% I_{ps}	0.45	0.65
Injector current (kA) for 50% I_{ps}	8.6	13.6
Maximum available injector flux (mWb)	80	340
Max. startup current potential (MA)	0.4	~1
Required injector current for max. current potential (kA)	10	27 ^a

^aHIT-II routinely operated with 30 kA injector current without impurity issues.

Previous analysis indicates that the neutral beam system should be capable of increasing the plasma current to the levels required for full non inductive operation¹⁴ starting from a plasma current of 500 kA. We assume that CHI will be capable of generating discharges with the same normalized internal plasma inductance of 0.35 at the nominal plasma radius of 0.93 m in NSTX-U. For these conditions, Eq. (3) yields an internal poloidal flux of 103 mWb. As seen in Table I, the toroidal flux in NSTX-U is much larger than in the present NSTX. Using Eq. (5), the current multiplication factor in NSTX-U is calculated to be 37, so to achieve 500 kA, the required injector current is 13.6 kA. If the initial lower inductance is lower, the peak CHI produced toroidal current could be expected to be higher: the peak toroidal current and the current multiplication factor could be up to 650 kA and 48, respectively.

The available injector flux for NSTX-U is considerably more than the enclosed poloidal flux in a full-current NSTX-U discharge. This improved current generation potential in NSTX-U is due to the much improved design of the CHI injector flux coil, which is positioned much closer to the CHI insulating gap. Note from Fig. 6 that the injector coil in NSTX is much farther away from the insulating gap so a smaller amount of the flux generated by this coil links the inner and outer divertor plates.

Although the injector flux capability in NSTX-U is large, the amount of useful injector flux defined as the amount of flux that can be injected with acceptable amount of low-Z impurities may be determined by electrode conditions. This is because a larger value of injector flux requires a higher level of injector current and this may increase the amount of impurity influx. Present NSTX experiments that have a graphite inner divertor electrode have been able to achieve injector current as large as 10 kA and these discharges when coupled to induction have successfully ramped to 1 MA. So this could be assumed to be a lower injector current bound on NSTX-U. Because the toroidal field on NSTX-U is nearly twice that in NSTX, the same value of injector current can inject nearly

twice the injector flux in NSTX-U. This should result in a lower bound on CHI produced toroidal current in NSTX-U on the order of 0.5 MA. If the injector current can be increased without creating additional impurity influx, toroidal currents up to 1 MA would be possible in NSTX-U.

V. SUMMARY AND CONCLUSIONS

Significant improvements to CHI performance in NSTX were achieved by reducing low-Z impurity influx into the plasma discharge and by applying additional “buffer” flux with a pair of absorber poloidal field coils to suppress absorber arcs. As a result, 300 kA of start-up current has been produced using just 29 kJ of stored capacitor bank energy. When these CHI started discharges are ramped up using induction, it is found that they require about 40% less inductive flux from the solenoid to reach 1 MA plasma current than inductive-only discharges. Furthermore, the resulting CHI started discharge has lower plasma density and normalized internal plasma inductance throughout the inductive ramp. Scaling to NSTX-U shows that CHI has the potential to generate nearly all of the initial current needed for subsequent non-inductive current sustainment by the bootstrap effect and neutral beam driven current. These results from NSTX demonstrate that CHI is a viable solenoid-free plasma startup method for advanced scenarios in future STs.

ACKNOWLEDGMENTS

We acknowledge the support of the NSTX team for operation of the machine systems and diagnostics. Special thanks are due to R. Hatcher, S. Ramakrishnan, and C. Neumeier for support with CHI related systems.

This manuscript has been authored by Princeton University and collaborators under Contract No(s). DE-AC02-09CH11466, DE-FG02-99ER54519 AM08, and DE-AC52-07NA27344 with the U.S. Department of Energy. The publisher, by accepting this article for publication, acknowledges that the United States Government retains a non-exclusive, paid-up, irrevocable, world-wide license to publish or reproduce the published form of this manuscript, or allow others to do so, for United States Government purposes.

¹M. Murakami, M. R. Wade, C. M. Greenfield, T. C. Luce, J. R. Ferron, H. E. St. John, J. C. DeBoo, W. W. Heidbrink, Y. Luo, M. A. Makowski, T. H. Osborne, C. C. Petty, P. A. Politzer, S. L. Allen, M. E. Austin, K. H. Burrell, T. A. Casper, E. J. Doyle, A. M. Garofalo, P. Gohil, I. A. Gorelov, R. J. Groebner, A. W. Hyatt, R. J. Jayakumar, K. Kajiwara, C. E. Kessel, J. E. Kinsey, R. J. La Haye, L. L. Lao, A. W. Leonard, J. Lohr, T. W. Petrie, R. I. Pinsker, R. Prater, T. L. Rhodes, A. C. C. Sips, G. M. Staebler, T. S. Taylor, M. A. Vanzeeland, G. Wang, W. P. West, L. Zeng, and the DIII-D Team, *Phys. Plasmas* **13**, 056106 (2006).

²T. R. Jarboe, *Plasma Phys. Controlled Fusion* **36**, 945 (1994).

³H. S. McLean, S. Woodruff, E. B. Hooper, R. H. Bulmer, D. N. Hill, C. Holcomb, J. Moller, B. W. Stallard, R. D. Wood, and Z. Wang, *Phys. Rev. Lett.* **88**, 125004 (2002).

⁴C. W. Barnes, T. R. Jarboe, G. J. Marklin, S. O. Knox, and I. Henins, *Phys. Fluids B* **2**, 1871 (1990).

⁵J. H. Hammer, J. L. Eddleman, C. W. Hartman, H. S. McLean, and A. W. Molvik, *Phys. Fluids B* **3**, 2236 (1991).

⁶Y. Ono, M. Yamada, T. Akao, T. Tajima, and R. Matsumoto, *Phys. Rev. Lett.* **76**, 3328 (1996).

⁷M. R. Brown, C. D. Cothran, D. Cohen, J. Horwitz, and V. Chaplin, *J. Fusion Energy* **27**, 16 (2008).

- ⁸M. Nagata, T. Kanki, N. Fukumoto, and T. Uyama, *Phys. Plasmas* **10**, 2932 (2003).
- ⁹R. Raman, T. R. Jarboe, D. Mueller, M. J. Schaffer, R. Maqueda, B. A. Nelson, S. A. Sabbagh, M. G. Bell, R. Ewig, E. D. Fredrickson, D. A. Gates, J. C. Hosea, S. C. Jardin, H. Ji, R. Kaita, S. M. Kaye, H. W. Kugel, L. L. Lao, R. Maingi, J. Menard, M. Ono, D. Orvis, F. Paoletti, S. F. Paul, Y.-K.M. Peng, C. H. Skinner, J. B. Wilgen, S. J. Zweben, and The NSTX Research Team, *Nucl. Fusion* **41**, 1081 (2001).
- ¹⁰R. Raman, T. R. Jarboe, B. A. Nelson, V. A. Izzo, R. G. O'Neill, A. J. Redd, and R. J. Smith, *Phys. Rev. Lett.* **90**, 075005 (2003).
- ¹¹R. Raman, D. Mueller, B. A. Nelson, T. R. Jarboe, S. Gerhardt, H. W. Kugel, B. LeBlanc, R. Maingi, J. Menard, M. Ono, S. Paul, L. Roquemore, S. Sabbagh, V. Soukhanovskii, and NSTX Research Team, *Phys. Rev. Lett.* **104**, 095003 (2010).
- ¹²T. R. Jarboe, *Fusion Technol.* **15**, 7 (1989).
- ¹³J. B. Taylor, *Rev. Mod. Phys.* **58**, 741 (1986).
- ¹⁴J. E. Menard, J. Canik, B. Covele, S. Kaye, C. Kessel, M. Kotschentreuther, S. Mahajan, R. Maingi, C. Neumeyer, M. Ono, R. Raman, S. Sabbagh, V. Soukhanovskii, and P. Valanju, *Physics Design of the NSTX-U*, **P2.106**, *Proceedings of the 27th EPS Conference on Plasma Physics*, Dublin, Ireland, 21–24 June (2010), Vol. 34A, ISBN 2-914771-62-2, <http://ocs.ciemat.es/EPS2010PAP/pdf/P2.106.pdf>.
- ¹⁵H. W. Kugel, M. G. Bell, J. W. Ahn, J. P. Allain, R. Bell, J. Boedo, C. Bush, D. Gates, T. Gray, S. Kaye, R. Kaita, B. LeBlanc, R. Maingi, R. Majeski, D. Mansfield, J. Menard, D. Mueller, M. Ono, S. Paul, R. Raman, A. L. Roquemore, P. W. Ross, S. Sabbagh, H. Schneider, C. H. Skinner, V. Soukhanovskii, T. Stevenson, J. Timberlake, W. R. Wampler, and L. Zakharov, *Phys. Plasmas* **15**, 056118 (2008).
- ¹⁶F. M. Levinton and H. Yuh, *Rev. Sci. Instrum.* **79**, 10F522 (2008).